9th ANKARA INTERNATIONAL AEROSPACE CONFERENCE **AIAC-2017-036**
20-22 September 2017 - METU, Ankara TURKEY

CFD ANALYSIS OF HELICOPTER ROTOR IN FORWARD FLIGHT

Ali Oğuz Yüksel[1]
Turkish Aerospace Industries, Inc.
Ankara, Turkey

Yusuf Özyörük[2]
Middle East Technical University
Ankara, Turkey

ABSTRACT

Objective of the study is to carry out flow solutions of helicopter rotors in forward flight. The study includes the solutions of both Euler and Reynolds Averaged Navier Stokes Equations in a time-dependent manner. Commercial software Ansys-Fluent 17.0 is used together with its User Defined Function (UDF) capability. A two-bladed Onera rotor model without cyclic motion and Caradonna-Tung rotor with cyclic motion are investigated. To assess the success of UDF for giving cyclic motion, comparisons with analytical blade motion is carried out. Chordwise pressure distributions at different spanwise sections are compared with the experimental and available numerical results from literature. Comparisons of the attained results show good agreement.

INTRODUCTION

Helicopters have more capability of maneuvering than fixed-wing aircrafts thanks to rotating wings. Motions of the helicopter provided by rotating wings might be divided into climbing, descending, hovering, forward flight and maneuvering which combines all motions. In all flight conditions, flow fields created by the helicopter rotor has complex structure because of vortex wake caused by wing tip and interaction of vortex wake with blade. However, forward flight calculations have additional challenges such as cyclic motions of blades, transonic flow over advancing blade tip, stall and reverse flow on retreating blade [Leishman, 2006]. In forward flight, sections of rotor blades are exposed to sectional velocity due to rotation and the component of forward flight velocity depending on azimuth angle. Thus, blade on the advancing side sees total of forward flight velocity and the velocity due to rotation. On the other hand, blade on the retreating side sees the velocity decreased by the forward flight velocity. If angle of attack were constant during rotation, advancing side of rotor create more lift than retreating side. Therefore, cyclic motions of blade is essential to balance roll moment. Figure 1 illustrates the critical definitions for rotor in forward flight [Johnson, 2013].

1 MSc. Student in Aerospace Engineering Department, Email: yuksel.ali@metu.edu.tr
2 Prof. in Aerospace Engineering Department, Email: yusuf.ozyoruk@ae.metu.edu.tr

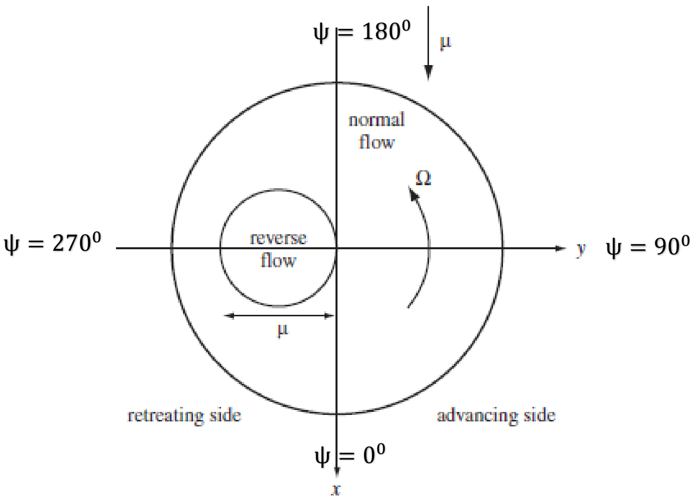

Figure 1: Definitions for rotor in forward flight

This work is a part of project which calculates the aeroacoustics noise of helicopter rotor in hover and forward flight [Özyörük, Yüksel, Ünal, 2016]. Calculations of aeroacoustics noise utilizes the computational fluid dynamics (CFD) analysis. In that purpose, flow field is accurately evaluated for helicopter rotor in hover [Yüksel, Özyörük, 2016]. In this work, CFD analysis are applied for helicopter rotor in forward flight. These analysis are performed in the two cases. The first is Onera two-bladed model rotor with no cyclic motion and the second is Caradonna and Tung rotor with cyclic motion [Steijl et al., 2006]. Cyclic motions are given by User Defined Functions (UDFs) which enhance Fluent's standard features [Ansys Inc., 2015]. UDFs are based on C programming language. After prescribed cyclic motion is accurately provided, transient analysis is performed by solving Euler and Navier-Stokes equations in each time step for the Onera two-bladed model rotor and Caradonna-Tung rotor, respectively. In the following chapters, method is stated; then, results are presented with comparisons and discussions.

METHOD

The flow fields around rotor in hover can be calculated in steady state manner. Moving reference frame (MRF) method transform the governing equations to the moving frame such that steady-state solutions are possible [Ansys Inc., 2015]. However, the forward flight with cyclic motions is a time-dependent problem. It includes not only steadily moving frame such as constant rotational speed but also flapping, pitching and lead-lag. Thus, transient simulation must be applied for the forward flight with cyclic motions.

Governing Equations

Compressible, three-dimensional, unsteady Reynolds Averaged Navier Stokes (RANS) equations are written in integral form as illustrated in the Equation 1.

$$\frac{d}{dt}\int_{\Omega(t)} \vec{w}\, d\Omega + \int_{d\Omega(t)} (\vec{F}\,(\vec{w}) - \vec{F}_v(\vec{w})).\vec{n}dA = \vec{S} \tag{1}$$

Conservation equations can be applied arbitrary control volume $\Omega(t)$ with boundary $d\Omega(t)$. Inviscid and viscous fluxes are $\vec{F}$ and $\overrightarrow{F_v}$, respectively. $\vec{w}$ represents $[\rho, \rho u, \rho v, \rho w, \rho E]^T$ vector. For cases in which MRF is used such as hovering rotor, the velocities are relative to the blade and therefore the source term is not zero. However, for transient analysis such as forward flight simulations in this work, the velocities are absolute and the right hand side source equals to zero [Steijl et al., 2006].

Mesh and Solution Strategies

The distance between rotation center and boundaries located at sides and top are 10 rotor radius. The bottom boundary is placed 15 rotor radius to the rotation center. Mesh refinement is performed in the regions of high gradient of flow, such as near tip vortex flow paths. The edge of the largest tetrahedron mesh in the mesh refinement region is taken about 0.15 chord. Figure 2 shows in different views the solution domain which is of cylindrical shape and the mesh refinement regions.

As boundary conditions, pressure far field boundary conditon is applied at far field boundaries, while no-slip wall condition is applied on the blades in viscous and no penetration condition in the inviscid simulation. Also for viscous flow simulation, wall y+ is set nearly equal to minimum 1, which is in the vicinity of blade tip. Spalart-Allmaras turbulence model is chosen as turbulence model.

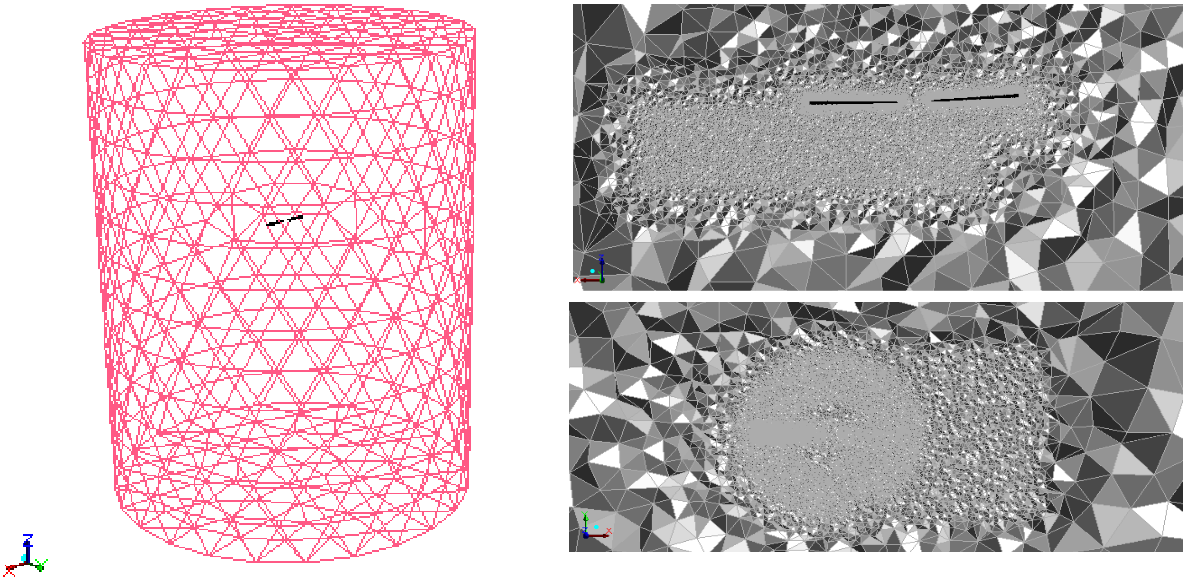

Figure 2: Solution domain and mesh refinement regions

Although pressure- based solvers are initially used for incompressible flows, the new modified versions of pressure-based solvers are applicable for a wide range of flow regimes from low speed incompressible flow to high-speed compressible flow. In this work, pressure based coupled solver (PBCS) is applied because PBCS decreases the time to reach convergence, approximately as much as five times, by solving momentum and pressure-based continuity equations in a coupled way [Keating, 2011]. Although PBCS requires about 2 times more memory, its advantages outweigh the weaknesses. Second order upwind discretization is used for in space, while dual time iteration strategy is employed with a subiterations number of 15, which ensured about 4 order of magnitude residual reduction at every physical time step. Time step for transient solution is 0.25 degree rotation of rotor. For transient simulations, mesh motion is required for each time step. Sliding mesh that does not include mesh deformation is enough for the forward flight without cyclic motion. However, sliding mesh and mesh deformation are used together for forward flight with cyclic motions in each time step. For forward flight with cyclic motion, rotation of the rotor is provided by sliding mesh; on the other hand, cyclic motions performed by UDF and mesh deformation. Cyclic motions of blade is applied on both blades and boundary layer. Thus, blade and boundary layers move together rigidly. This is beneficial in a variety of aspects. First is related to obtain positive volume for every mesh during transient analysis. Mesh in the boundary layer are very small elements. Hence, if only blades were in cyclic motion, mesh in the boundary layer overlap with blade which makes solution impossible. Second is the oscillation in solution. This oscillation is due to deformation of mesh around blades. On the other hand, when boundary layer and blades move rigidly together mesh deformation is minimal and away from the blades.

Cyclic Motions of Blade

Cyclic motions of blade which are flapping, pitching (feathering) and lead-lag are illustrated in the Equations 2, respectively. Therefore, flapping, pitching and lead-lag are depends on azimuth angle, which changes with time. These motions are given in order to balance asymetry of lift on the advancing and retreating sides of rotor disk.

$$\beta(\psi) = \beta_0 - \beta_{1c}\cos(\psi) - \beta_{1s}\sin(\psi)$$
$$\theta(\psi) = \theta_0 - \theta_{1c}\cos(\psi) - \theta_{1s}\sin(\psi) \qquad (2)$$
$$\zeta(\psi) = \zeta_0 - \zeta_{1c}\cos(\psi) - \zeta_{1s}\sin(\psi)$$
$$\psi(t) = \omega t$$

Time derivatives of the angles of the cyclic motion are the angular velocities around blade-fixed frame, which can be seen in Equations 3.

$$\dot{\beta} = -\beta_{1c}\omega\sin(\omega t) + \beta_{1s}\,\omega\cos(\omega t) \qquad (3)$$
$$\dot{\theta} = -\theta_{1c}\omega\sin(\omega t) + \theta_{1s}\,\omega\cos(\omega t)$$
$$\dot{\zeta} = -\zeta_{1c}\omega\sin(\omega t) + \zeta_{1s}\,\omega\cos(\omega t)$$

After angles of β_0, β_{1c}, β_{1s}, θ_0, θ_{1c}, θ_{1s}, ζ_0, ζ_{1c}, ζ_{1s} are appointed, positions of blades are known for all azimuth angles. Then, prescribed motions are given by UDF based on C programming language. The UDF macro requires the object on which the prescribed motion is applied and the angular velocities around Cartesian Coordinates (x, y, z). Therefore, the rotation matrices are required in order to acquire angular velocities around Cartesian Coordinates from angular velocities around blade-fixed frame $\beta(\dot{\psi})$, $\theta(\dot{\psi})$, $\zeta(\dot{\psi})$. Equations 4 shows the rotation matrices.

$$R_1 = \begin{bmatrix} \cos(\psi) & -\sin(\psi) & 0 \\ \sin(\psi) & \cos(\psi) & 0 \\ 0 & 0 & 1 \end{bmatrix} \qquad R_2 = \begin{bmatrix} \cos(\beta) & 0 & -\sin(\beta) \\ 0 & 1 & 0 \\ \sin(\beta) & 0 & \cos(\beta) \end{bmatrix}$$

$$R_3 = \begin{bmatrix} \cos(\zeta) & -\sin(\zeta) & 0 \\ \sin(\zeta) & \cos(\zeta) & 0 \\ 0 & 0 & 1 \end{bmatrix} \qquad R_4 = \begin{bmatrix} 1 & 0 & 0 \\ 0 & \cos(\theta) & -\sin(\theta) \\ 0 & \sin(\theta) & \cos(\theta) \end{bmatrix} \qquad (4)$$

Assume that rotation centers of cyclic motions (flapping, pitching and lead-lag) are the same as rotation center of rotor, Equations 5 illustrates the how to use the transformation matrices in order to obtain angular velocities around Cartesian Coordinates. Hence, cyclic motions of blades are provided by UDF with input data including angles of cyclic motions.

$$\begin{bmatrix} \omega_x \\ \omega_y \\ \omega_z \end{bmatrix} = R_4 R_3 R_2 R_1 \begin{bmatrix} \dot{\theta} \\ 0 \\ 0 \end{bmatrix} + R_3 R_2 R_1 \begin{bmatrix} 0 \\ 0 \\ \dot{\zeta} \end{bmatrix} + R_2 R_1 \begin{bmatrix} 0 \\ -\dot{\beta} \\ 0 \end{bmatrix} \qquad (5)$$

As mentioned earlier, UDF provides the cyclic blade motions causing mesh deformation; on the other hand, rotation of the rotor is provided by sliding mesh in forward flight with cyclic motion. Time step size is 0.25 degree of rotor rotation for all these motions. Hence, motions are provided numerically. In order to validate numerical motion provided by UDF and sliding mesh, analytical calculation is written in Fortran 90. For the analytical calculation, an arbitrary

(6)

point on blade is exposed to rotation matrices as illustrated in Equation 6. Hence, an arbitrary point (x_i, y_i, z_i) reaches the final position (x_f, y_f, z_f).

$$\begin{bmatrix} x_f \\ y_f \\ z_f \end{bmatrix} = R_4 R_3 R_2 R_1 \begin{bmatrix} x_i \\ y_i \\ z_i \end{bmatrix}$$

RESULTS and DISCUSSIONS

Onera two-bladed model rotor in forward flight without cyclic motion

The main object of this work is to perform accurate CFD analysis for rotor in forward flight with cyclic motion. In that purpose, forward flight without cyclic motion initially performed in order to prepare for cyclic motion case. Onera two-bladed model rotor shown in Figure 3 is considered. Radius of rotor is 0.75 m and length of root chord is 0.166 m.

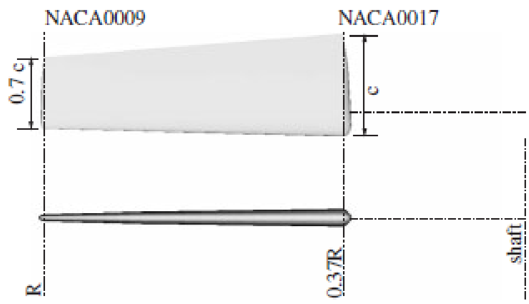

Figure 3: Geometry of Onera model rotor blade

Forward flight Mach Number is 0.3125 and advance ration is 0.5. Hence, transonic flow occurs at advancing side of rotor. Inviscid flow solution gives the accurate results because in that flow regime, inertial forces dominates the viscous forces. Hence, Solution of Euler Equations are cost efficient. Therefore, Euler equations are solved for this case. The results illustrated in Figure 4 are acquired after 2 revolutions are completed. Although the beginning position of the shock is predicted slightly late or early, the maximum difference between shock starting point in the analysis and experiment is 0.05c that is 8mm. Therefore, the results of pressure distributions along chord are consistent with experiment [Philippe, Chattot, 1980].

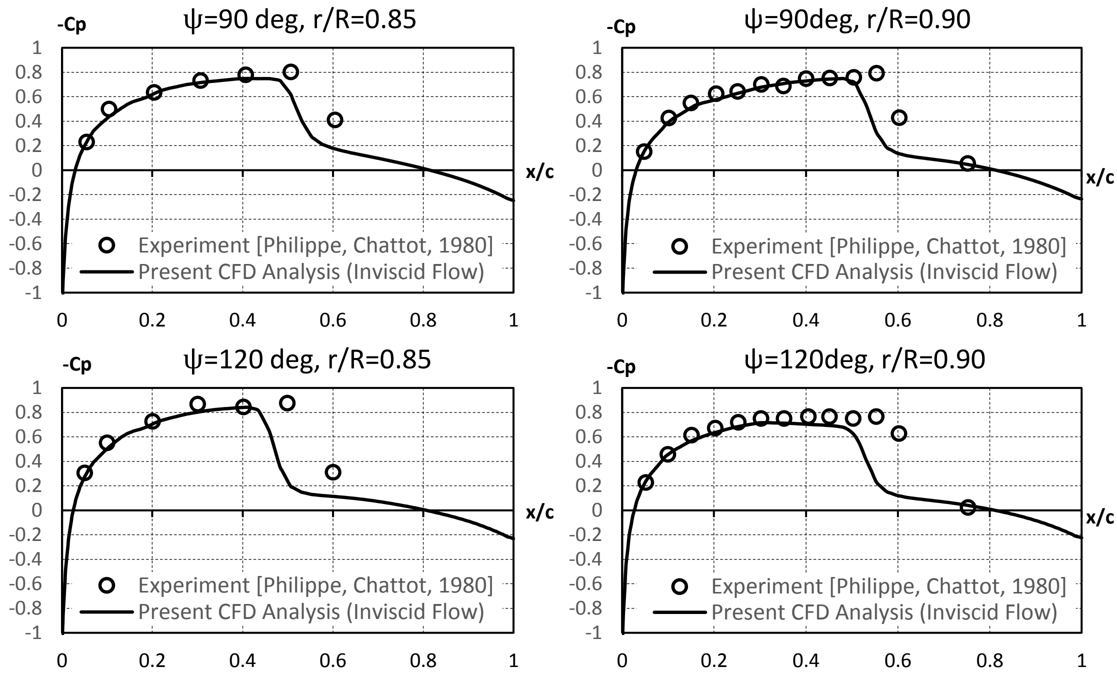

Figure 4: Pressure coefficient distribution along chord for different spanwise sections

Caradonna-Tung rotor in forward flight with cyclic motion

Time-dependent simulation of Caradonna-Tung rotor with 2 blades in forward flight with cyclic motion is performed when forward flight Mach Number is equal to 0.15 and advance ratio is 0.25. Prescribed flapping, pitching and lead-lag angles are defined in Table 1.

Table 1: Angles of the cyclic motion

θ_0	θ_{1s}	θ_{1c}	β_0	β_{1s}	β_{1c}	ζ_0	ζ_{1s}	ζ_{1c}
4.0^o	2.0^o	0.0^o	1.5^o	2.0^o	2.0^o	0.0^o	-2.0^o	0.0^o

Before comparison of pressure distributions along chord, validation of the motion is performed. Analytical calculation is compared with numerical calculation as stated in Chapter Method. In that purpose, a point on the blade tip is exposed to numerical and analytical cyclic motion. Figure 5 shows the difference between numerical and analytical deflections over maximum deflection during two revolutions. Difference over maximum deflection is about 0.006. This means the distance between numerical and analytical cyclic motion is approximately 0.5mm that is good agreement. Therefore, it is stated that UDF gives the cyclic motion and rotation accurately.

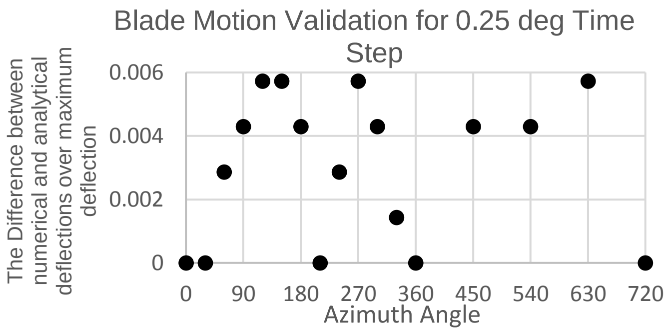

Figure 5: Analytical and numerical cyclic motion comparison

Sliding mesh is applied on whole domain and UDF gives boundary layer and blades the cyclic motion. Mesh elements out of the boundary layer is exposed to mesh deformation due to cyclic motion. Pressure contours on the blades is obtained for azimuth angles of $30^o, 90^o$, 150^o 210^o, 270^o, 330^o as illustrated in Figure 6. Flow direction is from x-negative to x-positive.

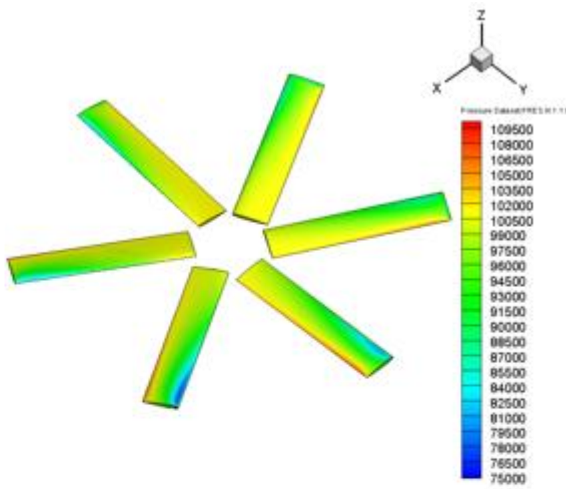

Figure 6: Pressure contours on a blade at various azimuthal angles

Convergence plays crucial role to obtain accurate results. During solution process, forces produced by rotor in upward direction (+z) and in flow direction (+x) are normalized. Because the two rotor is included this case, it is expected to periodic motion in each 180 deg rotation. Figure 7 represents this periodic motion during last 2 revolution, which is forth and fifth one.

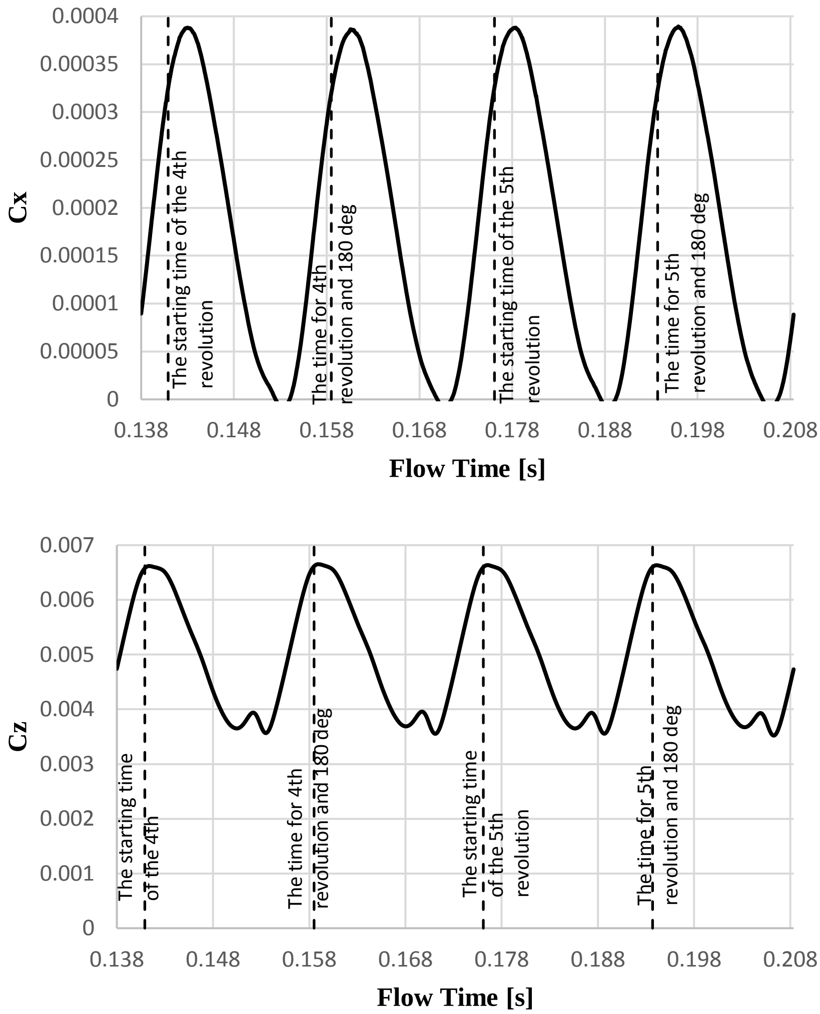

Figure 7: Normalized forces for 4th and 5th revolution

Pressure distributions along chord at r/R=0.89 is compared with the other analysis. Comparison of the viscous flow simulations of rotor in forward flight with cyclic motion is shown in Figure 8. It shows very good agreement between the viscous CFD analysis in this work and the viscous solution of Steijl et al. (Steijl et al., 2006).

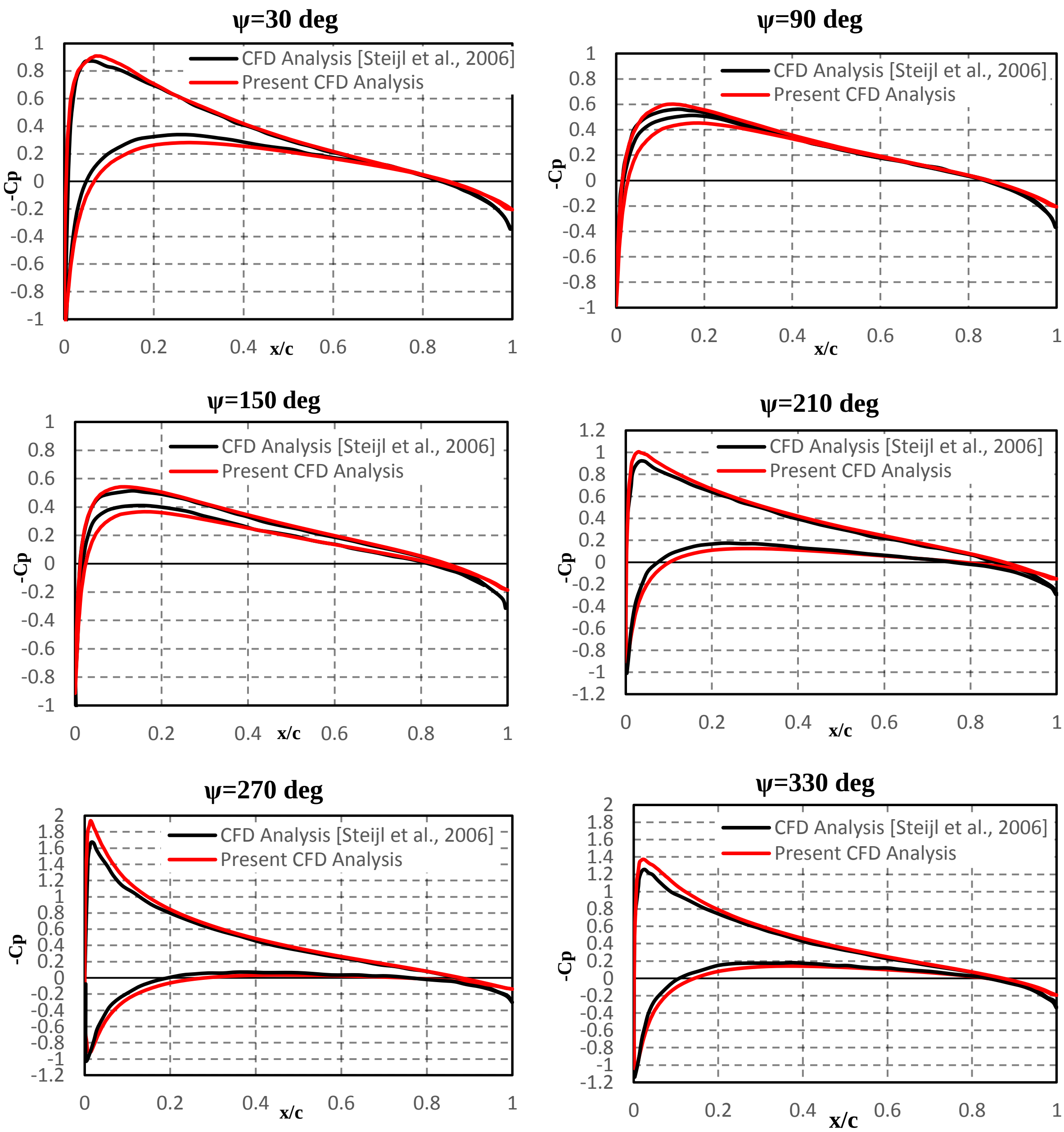

Figure 8: Comparison of pressure distributions along chord at r/R=0.89

This paper is concern with Navier Stokes simulations of helicopter rotor in forward flight. Simulations were carried out using commercial software Fluent 17. Two different rotor cases were solved, one without cyclic motion, the other with a cyclic motion of flapping, pitching and lead-lagging. Results were compared with available data with the literature with good agreement.

ACKNOWLEDGEMENT

This work is supported by Undersecretariat for Defence Industries (SSM), Turkish Aerospace Industries, Inc. (TAI) through Rotary Wing Technology Center (DKTM).

References

Ansys Inc., (2015) *Fluent User's Guide: Flows with Moving Reference Frames, Flows Using Sliding and Dynamic Meshes.*

Johnson, W., (2013) *Rotorcraft Aeromechanics*, Cambridge University Press, p: 30-31, 152-161.

Keating, M., (2011) *Accelerating CFD Solutions*, ANSYS Advantage.

Leishman, J.G. (2006) *Principles of Helicopter Aerodynamics,* Cambridge University Press, p: 171-185.

Özyörük, Y., Yüksel, O. and Ünal, A., (2016) *Helikopter Aerodinamik Gürültüsü Hesaplamaları için Yazılım Geliştirilmesi, İlerleme Raporu 4,* TUSAŞ-DKTM, June 2016.

Philippe, J. J., Chattot, J. J., (1980) *Experimental and Theoretical Studies on Helicopter Blade Tips at ONERA.* Sixth European Rotorcraft and Powered Lift Aircraft Forum, September 1980.

Steijl, R., Barakos, G. and Badcock, K., (2006) *A framework for CFD Analysis of Helicopter Rotors in Hover and Forward Flight,* International Journal for Numerical Methods in Fluids 2006; 51:819-847, January 2006.

Yüksel, A. O. and Özyörük Y. (2016) *Askı Uçuşundaki Helikopter Rotorunun Akış Alanı Hesaplamaları, National Aerospace Conference (UHUK), September 2016.*